$Sr_{11}Cd_6Sb_{12}$: a new Zintl compound with infinite chains of pentagonal tubes

Seon-Mi Park and Sung-Jin Kim*

Department of Chemistry/Division of Nano Sciences, Ewha Womans University, 11-1 Daehyon-Dong Soaemun-Ku, Seoul 120-750, South Korea

Abstract

A new Cd-containing transition metal Zintl phase, $Sr_{11}Cd_6Sb_{12}$, was obtained from a direct element combination reaction using the Sn flux method. Its structure was determined using single-crystal X-ray diffraction methods. It crystallizes in the monoclinic space group $C2/m$ with $a = 32.903(3)$ Å, $b = 4.7666(5)$ Å, $c = 12.6057(13)$ Å, $\beta = 109.752(2)°$, and $Z = 2$. $Sr_{11}Cd_6Sb_{12}$ has a one-dimensional infinite chain structure consisting of double pentagonal tubes, where Sr^{2+} cations reside both within two tubes and between the infinite chains of tubes. The anionic framework $[Cd_6Sb_{12}]^{22-}$ has features similar to those of $Eu_{10}Mn_6Sb_{13}$. The difference in $Eu_{10}Mn_6Sb_{13}$ is that its double pentagonal tubes are further condensed to form two-dimensional layers.
© 2004 Elsevier Inc. All rights reserved.

Keywords: Zintl phase; $CdSb_4$ tetrahedra; Ternary antimonide; Double pentagonal tubes

1. Introduction

The number of transition-metal-containing Zintl compounds has grown gradually over the last decade due to both their unique structures and their unusual magnetic properties [1–11]. Recently, we have been working with the new transition metal Zintl compounds $Eu_{10}Mn_6Sb_{13}$ [12] and Sr_2MnSb_2 [13]. Generally, the chemical behavior of Mn is known to be similar to that of Cd and Zn, as can be seen in $Ca_9Zn_4Bi_9$–$Ca_9Mn_4Bi_9$ [14] and $Ca_{14}CdSb_{11.43}$–$Ca_{14}MnSb_{11}$ [15,16]. In an attempt to synthesize an air-stable analogue of Sr_2MnSb_2, we tried to substitute Sr and Mn atoms with other heavy elements, such as Eu and Cd atoms. Consequently, the Eu substitution reaction yielded $Eu_{10}Mn_6Sb_{13}$ [12] and the Cd substitution reaction the new Zintl compound $Sr_{11}Cd_6Sb_{12}$, which is also air sensitive. The structure of $Sr_{11}Cd_6Sb_{12}$ and $Eu_{10}Mn_6Sb_{13}$ are commonly composed of corner- and edge-sharing Cd or Mn-centered tetrahedra forming double pentagonal tubes. However, the structure of Sr_2MnSb_2 is composed of corrugated layers of corner-

and edge-shared Mn-centered tetrahedral forming rhombic tubes.

Ternary Cd-containing antimonides have so far been the subject of little investigation. Most reports on the crystal structures of Cd-containing Zintl compounds have been performed on ACd_2Sb_2 (A = Ca, Sr, Ba, Eu, Yb) [17–19], which crystallizes in $CaAl_2Si_2$-type structure. The others, $LaCd_{0.7}Sb_2$ [20] and $NaCdSb$ [21], are composed of $CdSb_4$ tetrahedra sharing their corners or edges with each other, and $Ca_{14}CdSb_{11.43}$, which is composed of isolated $CdSb_4$ tetrahedron and isolated Sb atoms with $Ca_{14}AlSb_{11}$ type [22]. Here we report on the synthesis and crystal structure of $Sr_{11}Cd_6Sb_{12}$ as contrasted with that of $Eu_{10}Mn_6Sb_{13}$.

2. Experimental section

2.1. Synthesis

$Sr_{11}Cd_6Sb_{12}$ was synthesized from the elements Sr (Aldrich, chips, 99.9%), Cd (Aldich, powder, 99.9%), and Sb (High purity, powder, 99.999%), using a Sn (Junsei, drops, 99.9%) flux method. All manipulations were performed in a N_2-filled glove box. The mixture of

*Corresponding author. Fax: +82-2-3277-2384.
  E-mail address: sjkim@ewha.ac.kr (S.-J. Kim).

elements (Sr:Cd:Sb:Sn = 10:6:11:30) was placed in a graphite tube, which was then vacuum sealed in a quartz tube. The mixture was heated to 1000°C at a rate of 10°C/h, held at 1000°C for 24 h, cooled to 550°C at 5°C/h, held at 550°C for 4 days, and then cooled to room temperature at 5°C/h. After the reaction, to remove excess Sn flux from the product, SiO_2 wool was inserted into a long quartz tube where a carbon tube-containing product was placed, and then the quartz tube was evacuated and sealed. The sealed reaction tube, where the product was placed on top, was put upright in a box furnace and heated to 500°C at a rate of 100°C/h, and kept at that temperature for 2 h, thereafter, this tube was moved from the furnace to a centrifuge and spun immediately, and then the excess Sn flux was gathered at the bottom of tube. A black chunk, single crystal of $Sr_{11}Cd_6Sb_{12}$ was treated in a N_2-filled glove box because of the instability in the air. A semi-quantitative micro-probe analysis on the single crystals gave $Sr_{11.2(2)}Mn_{5.8(1)}Sb_{12.2(2)}$ (an average of three data acquisitions). Once the stoichiometry was determined from X-ray single-crystal structure analysis, the $Sr_{11}Cd_6Sb_{12}$ was prepared rationally as a single phase, starting from the exact stoichiometric ratio using same temperature profile.

2.2. Electron microscopy

A semi-quantitative microprobe analysis of the compounds was performed using a JEOL JSM-35C scanning electron microscope equipped with a Tracor Northern energy dispersive spectroscopy detector. Data were acquired using an accelerating voltage of 20 kV and a 30-s accumulation time.

2.3. Crystallographic studies

A single-crystal X-ray analysis was carried out using a Bruker SMART Platform CCD diffractometer on a black crystal with a dimension of $0.22 \times 0.14 \times 0.06$ mm^3. This moisture-sensitive crystal was dipped in paratone oil and picked up with a glass fiber, and then inserted into a thin-walled 0.3 mm diameter glass capillary. The capillary was purged with nitrogen gas, and then sealed with a small torch. The data set was collected over a half sphere of reciprocal space up to 56° in 2θ at 233(2) K under a nitrogen cold stream. The individual frames were measured with a ω rotation of 0.3° and an acquisition time of 30 s. To check the stability of the crystal, at the end of the data collection procedure the initial 50 frames of data were measured again and compared. No crystal decay was detected. The SMART software was used for data acquisition and SAINT for data extraction and reduction. The absorption correction was performed empirically using SA-DABS. The observed Laue symmetry and systematic extinctions were indicative of the space group $C2/m$ and

Table 1
Selected data from the single-crystal structure refinement of $Sr_{11}Cd_6Sb_{12}$

Empirical formula	$Sr_{11}Cd_6Sb_{12}$
Formula weight	3099.22
Temperature (K)	233(2)
Wavelength ($\lambda = K\alpha$, Å)	0.71073
Crystal system	Monoclinic
Space group	$C2/m$ (no. 12)
Unit-cell dimensions (Å)	$a = 32.903(3)$
	$b = 4.7666(5)$
	$c = 12.6057(13)$
	$\beta = 109.752(2)°$
Volume (Å^3)	1860.7(3)
Z	2
Density, ρ_{calc} (g/cm^3)	5.532
Absorption coefficient (mm^{-1})	27.486
Reflections collected/unique	5928/2500 [$R_{(int)} = 0.0377$]
Data/restrains/parameters	2500/0/89
Final R indices [$F_o^2 > 2\sigma(F_o^2)$][a]	$R_1 = 0.0523$, w$R_2 = 0.1175$
R indices ($F_o^2 > 0$)	$R_1 = 0.0637$, w$R_2 = 0.1244$
Largest diff. peak and hole(e/Å^3)	2.621 and -4.508

[a] $R_1 = [\sum |F_o| - |F_c|]/\sum |F_o|$, w$R_2 = \{[\sum w[(F_o)^2 - (F_c)^2]^2]/[\sum w(F_o^2)^2]\}^{1/2}$ for $F_o^2 > 2\sigma(F_o^2)$, w$= [\sigma^2(F_o)^2 + (0.0699)P^2 + 45.1240P]^{-1}$, where $P = (F_o^2 + 2F_c^2)/3$.

Table 2
Atomic coordinates ($\times 10^4$) and equivalent isotropic displacement parameters (Å$^2 \times 10^3$) for $Sr_{11}Cd_6Sb_{12}$

Atom	Wyckoff position	x	y	z	U(eq)[a]
Sr(1)	4i	4814(1)	−5000	3189(1)	10(1)
Sr(2)	4i	1997(1)	0	3427(1)	11(1)
Sr(3)	4i	3863(1)	−5000	4938(1)	9(1)
Sr(4)	4i	2785(1)	0	1326(1)	12(1)
Sr(5)	2a	0	0	0	9(1)
Sr(6)	4i	1260(1)	0	164(1)	11(1)
Sb(1)	4i	3087(1)	0	4677(1)	9(1)
Sb(2)	4i	895(1)	0	2331(1)	9(1)
Sb(3)	4i	3506(1)	−5000	2173(1)	8(1)
Sb(4)	4i	4571(1)	0	4985(1)	8(1)
Sb(5)	4i	2050(1)	−5000	1356(1)	9(1)
Sb(6)	4i	4538(1)	0	1164(1)	8(1)
Cd(1)	4i	3997(1)	0	2541(1)	11(1)
Cd(2)	4i	2810(1)	−5000	3326(1)	12(1)
Cd(3)	4i	477(1)	−5000	2446(1)	16(1)

[a] U(eq) is defined as one-third of the trace of the orthogonalized U_{ij} tensor.

$C2$. The centrosymmetric space group $C2/m$ was assumed, and subsequent refinements confirmed this space group. The final cycle of refinement performed on F_o^2 with 89 variables and 2500 averaged reflections converged to the residuals wR_2 ($F_o^2 > 0$) = 0.1244. The conventional R index based on reflections having $F_o^2 > 2\sigma(F_o^2)$ was 0.0523. The final difference Fourier synthesis map showed maximum and minimum peaks of 2.621 and -4.508 e/Å^3, respectively. The complete data collection parameters and details of the structure solution and refinement results for the two different

Table 3
Selected bond distances (Å) and angles (deg) for $Sr_{11}Cd_6Sb_{12}$

Cd(1)–Sb(3) × 2	2.8269(9)	Sr(3)–Sb(1) × 2	3.4242(14)
Cd(1)–Sb(4)	3.0208(16)	Sr(3)–Sb(2)	3.2605(18)
Cd(1)–Sb(6)	2.8774(16)	Sr(3)–Sb(3)	3.2805(18)
Cd(2)–Sb(1) × 2	2.8918(9)	Sr(3)–Sb(4) × 2	3.3191(13)
Cd(2)–Sb(3)	3.0999(17)	Sr(3)–Cd(2)	3.371(2)
Cd(2)–Sb(5)	2.8672(16)	Sr(4)–Sb(3) × 2	3.2767(13)
Cd(3)–Sb(2) × 2	2.7789(9)	Sr(4)–Sb(5) × 2	3.4041(14)
Cd(3)–Sb(4)	3.2941(18)	Sr(4)–Sb(5)	3.600(2)
Cd(3)–Sb(6)	2.9641(17)	Sr(4)–Cd(1)	3.756(2)
Sb(4)–Sb(4)	2.814(2)	Sr(4)–Cd(2) × 2	3.4498(15)
Sr(1)–Sb(4) × 2	3.4545(13)	Sr(5)–Sb(2)	3.3837(11)
Sr(1)–Sb(4) × 2	3.5599(14)	Sr(5)–Sb(6) × 4	3.4134(8)
Sr(1)–Sb(6) × 2	3.3844(13)	Sr(5)–Cd(3) × 4	3.7920(11)
Sr(1)–Cd(1) × 2	3.4769(15)	Sr(6)–Sb(2)	3.3362(18)
Sr(1)–Cd(3) × 2	3.5643(16)	Sr(6)–Sb(3)	3.2861(18)
Sr(2)–Sb(1)	3.3954(19)	Sr(6)–Sb(5) × 2	3.4726(14)
Sr(2)–Sb(1) × 2	3.4522(14)	Sr(6)–Sb(6) × 2	3.5218(14)
Sr(2)–Sb(2)	3.4185(19)		
Sr(2)–Sb(5) × 2	3.5832(14)	Sb(5)–Cd(2)–Sb(1)	121.29(3)
Sr(2)–Cd(2) × 2	3.6169(15)	Sb(1)–Cd(2)–Sb(1)	111.01(5)
		Sb(5)–Cd(2)–Sb(3)	99.20(5)
Sb(3)–Cd(1)–Sb(3)	114.93(6)	Sb(1)–Cd(2)–Sb(3)	98.05(4)
Sb(3)–Cd(1)–Sb(6)	109.64(4)	Sb(2)–Cd(3)–Sb(2)	118.10(6)
Sb(3)–Cd(1)–Sb(4)	107.03(4)	Sb(2)–Cd(3)–Sb(6)	114.46(3)
Sb(6)–Cd(1)–Sb(4)	108.33(5)	Sb(2)–Cd(3)–Sb(4)	103.88(4)
		Sb(6)–Cd(3)–Sb(4)	98.57(5)

Fig. 1. A view of the crystal structures of (a) $Sr_{11}Cd_6Sb_{12}$ and (b) $Eu_{10}Mn_6Sb_{13}$ down the *b*-axial direction showing the unit-cell outline. The Cd and Mn atoms are indicated as green and blue circles, and the Sb atoms are yellow circles, respectively. The Sr and Eu atoms in each compound are shown in red circles. A part of the structure is presented in a polyhedron model showing the corner and edge sharing of the Mn-centered tetrahedral.

temperatures are given in Table 1. The final atomic positions and isotropic thermal parameters are provided in Table 2. The selected bond distances and angles are listed in Table 3.

3. Results and discussion

The structure of $Sr_{11}Cd_6Sb_{12}$ is an anisotropic infinite one-dimensional structure composed of double pentagonal tubes. The overall structure of this compound, projected along the *b* axis, is shown in Fig. 1(a). The infinite chains of $[Cd_6Sb_{12}]^{22-}$ running along the *b*-axis have a covalent Cd/Sb network of $CdSb_4$ tetrahedra and are separated by Sr^{2+} cations. Among six crystallographically different Sr atoms, the Sr(1) atoms are filled in pentagonal tubes composed of Sb and Cd atoms while the others are between the anionic infinite chains.

As shown in Fig. 1(b), the structural feature of previously reported $Eu_{10}Mn_6Sb_{13}$ is similar to that of $Sr_{11}Cd_6Sb_{12}$. The structure of $Eu_{10}Mn_6Sb_{13}$ is made up of double layers of Mn-centered tetrahedral, and Eu^{2+} atoms separate the double layers. These double layers are composed of edge- and corner-sharing Mn-centered tetrahedra that form cavities occupied by Eu^{2+} cations and $[Sb_2]^{4-}$ dumbbells [12]. In the two compounds the basic pattern of condensed tetrahedra featuring double pentagonal tubes is similar. However, firstly, the difference in $Eu_{10}Mn_6Sb_{13}$ is that the two Mn-centered tetrahedral, Mn(2) and Mn(4), attached on the double
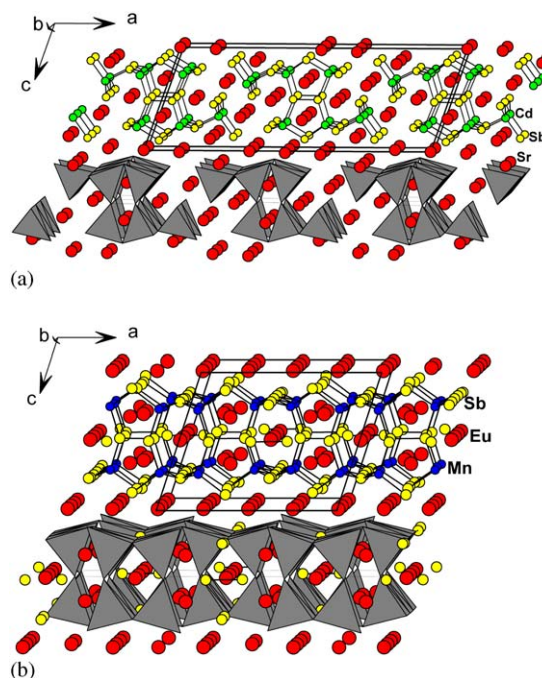
pentagonal tube are further condensed by sharing tetrahedral edges of Sb atoms to form two-dimensional double-layered structures, as shown in Fig. 2(b). Secondly, while Sb(4) and Sb(6) atoms of Cd(1)- and Cd(3)-centered tetrahedra are bridged or shared to form pentagonal double tubes in $Sr_{11}Cd_6Sb_{12}$, Sb(1), Sb(3), and Sb(6) atoms of Mn(1)- and Mn(2)-centered tetrahedra are not fully connected and thus cannot form double tubes in $Eu_{10}Mn_6Sb_{13}$.

In Zintl phases, if the electronegative element receiving electrons from the electropositive element does not fulfill the octet requirements, more complicated covalent polyanionic structures are formed via sharing ligands. A comparison of the $[Mn_{12}Sb_{24}]^{36-}$ anionic network excluding an isolated dimer $(Sb_2)^{4-}$ in $Eu_{10}Mn_6Sb_{13}$ and $[Cd_{12}Sb_{24}]^{44-}$ in $Sr_{11}Cd_6Sb_{12}$ indicates a relative abundance of electrons in $[Cd_{12}Sb_{24}]^{44-}$, thus suggesting less condensation of tetrahedra in $Sr_{11}Cd_6Sb_{12}$. The Sb atoms in $Sr_{11}Cd_6Sb_{12}$ have a 1-, 2-, and 3-coordinated environment, and those in $Eu_{10}Mn_6Sb_{13}$ have a 1-, 2-, 3-, and 4-coordinated environment; this confirms a more covalent condensation of Sb ligands in $Eu_{10}Mn_6Sb_{13}$.

As shown in Fig. 2(a), there are three crystallographically different Cd atoms in the anionic framework $[Cd_6Sb_{12}]^{22-}$. The double pentagon tubes are
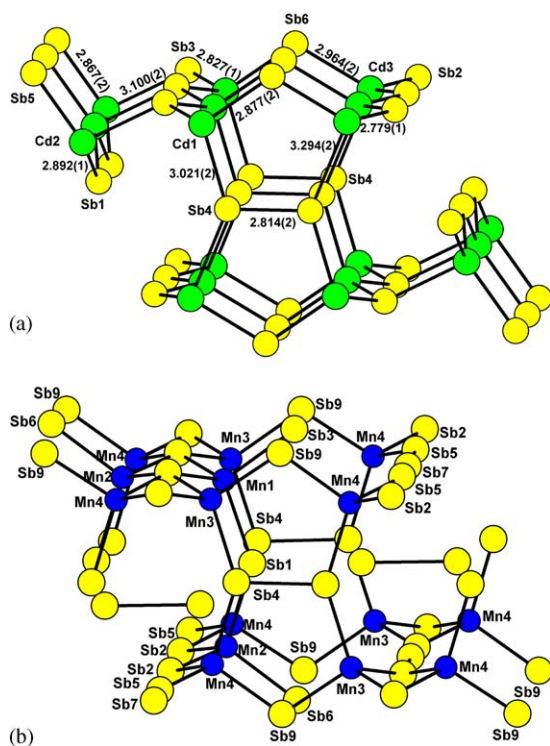
Fig. 2. A fragment of the anionic framework (a) $[Cd_6Sb_{12}]^{22-}$ in $Sr_{11}Cd_6Sb_{12}$ and (b) $[Mn_6Sb_{13}]^{20-}$ in $Eu_{10}Mn_6Sb_{13}$. The Cd and Mn atoms are indicated green and blue circles, and the Sb atoms are yellow circles, respectively. For comparison, a fragment of $[Mn_6Sb_{13}]^{20-}$ with a double pentagonal tube in $Eu_{10}Mn_6Sb_{13}$ is shown. In $Eu_{10}Mn_6Sb_{13}$, the two Mn-centered tetrahedra, Mn(2) and Mn(4), attached on the double pentagonal tube, are further condensed by sharing tetrahedral edges of Sb atoms to form a two-dimensional double-layered structure.

formed by a corner sharing of Cd(1)- and Cd(3)-centered tetrahedra and the Sb_2 bridge. Cd(2)-centered tetrahedra are in trans-direction to the double pentagon tubes. The tetrahedral angles around the Cd atoms are in a range of $107.03(4)° \sim 114.93(6)°$ for Cd(1), $98.05(4)° \sim 121.29(3)°$ for Cd(2), and $98.57(5)° \sim 118.10(6)°$ for Cd(3). The Cd(2) displays the most distorted environment compared to the ideal tetrahedral angle. This indicates that the geometry around the Cd atom depends on the extent of the sharing occurring between Sb atoms with their neighboring Cd atoms. The Cd(2), with its highly distorted environment, shares only one Sb atom with Cd(1), Cd(1) shares all Sb atoms with its neighboring Cd(2) and Cd(3), and Cd(3) shares two Sb atoms with its neighboring Cd(2). The Sb–Sb bond distance of dumbbell $[Sb_2]^{4-}$ is 2.814(2) Å, which seems to be a regular covalent bond and is comparable to those found in $Eu_5In_2Sb_6$ (2.861(4) Å) [23] and $Eu_{10}Mn_6Sb_{13}$ (3.074(3) Å) [12]. The observed Cd–Sb distances range from 2.779(1) to 3.294(2) Å. Especially, Cd(3) has the shortest and longest distances to Sb atoms among all Cd–Sb distances. The average of Cd–Sb distances, except for the two extremes at 2.779(1) and 3.294(2) Å,

is 2.918(2) Å, which is in good agreement with the data on previously reported Cd-containing Zintl compounds $SrCd_2Sb_2$ (2.872 Å, 2.972 Å) [17], NaCdSb (2.864 Å, 2.977 Å) [21], and $LaCd_{0.7}Sb_2$ (2.899 Å) [20].

According to the Zintl concept, the formal charge of three-bonded Sb atoms can be assigned as Sb^0, that of the two-bonded Sb atoms as Sb^{1-}, and that of the one-bonded Sb atoms as Sb^{2-}. In the case of the four-coordinated Cd atom, two extra electrons are needed to fulfill the octet rule. Therefore, it can be assigned as Cd^{2-} according to the Zintl concept. Consequently, the compound can be described as the valence-precise compound $(Sr^{2+})_{11}[(Cd^{2-})_6(1bSb^{2-})_2(2bSb^{1-})_6(3bSb^0)_4]$. However, the formal oxidation state can be described as $(Sr^{2+})_{11}[(Cd^{2+})_6(Sb^{3-})_{10}(Sb_2^{4-})]$. This $Sr_{11}Cd_6Sb_{12}$ is a new addition to the family of transition metal Zintl phases, and can extend the Zintl concept as a useful tool in rationalizing the stability of a covalent framework.

Acknowledgments

References

[1] S.M. Kauzlarich (Ed.), Chemistry, Structure, and Bonding of Zintl Phases and Ions, VCH Publishers, Inc.: New York, 1996 (Chapter 6).

[2] J.Y. Chan, S.M. Kauzlarich, P. Klavins, J.-Z. Liu, R.N. Shelton, D.J. Webb, Phys. Rev. B 61 (2000) 459.

[3] J.Y. Chan, S.M. Kauzlarich, P. Klavins, R.N. Shelton, D.J. Webb, Chem. Mater. 9 (1997) 3132.

[4] J.Y. Chan, S.M. Kauzlarich, P. Klavins, R.N. Shelton, D.J. Webb, Phys. Rev. B 57 (1998) 8103.

[5] H. Kim, J.Y. Chan, M.M. Olmstead, P. Klavins, D.J. Webb, S.M. Kauzlarich, Chem. Mater. 14 (2002) 206.

[6] D. Sánchez-Portal, R.M. Martin, S.M. Kauzlarich, W.E. Pickett, Phys. Rev. B 65 (2002) 144414.

[7] A.P. Holm, S.M. Kauzlarich, S.A. Morton, G.D. Waddill, W.E. Pickett, J.G. Tobin, J. Am. Chem. Soc. 124 (2002) 9894.

[8] H. Kim, C.L. Condron, A.P. Holm, S.M. Kauzlarich, J. Am. Chem. Soc. 122 (2000) 10720.

[9] F. Gascoin, S.C. Sevov, Angew. Chem. Int. Ed. 41 (2002) 1232.

[10] F. Gascoin, S.C. Sevov, Inorg. Chem. 41 (2002) 2820.

[11] F. Gascoin, S.C. Sevov, Inorg. Chem. 41 (2002) 5920.

[12] A.P. Holm, S.-M. Park, C.L. Condron, H. Kim, P. Klavins, F. Grandjean, R.P. Hermann, G.J. Long, M.G. Kanatzidis, S.M. Kauzlarich, S.-J. Kim, Inorg. Chem. 42 (2003) 4660.

[13] S.-M. Park, S.-J. Kim, M.G. Kanatzidis, in preparation.
[14] E. Brechtel, G. Cordier, H. Schäfer, Z. Naturforsch. 34B (1979) 1229.
[15] D.M. Young, C.C. Torardi, M.M. Olmstead, S.M. Kauzlarich, Chem. Mater. 7 (1995) 93.
[16] A. Rehr, T.Y. Kuromoto, S.M. Kauzlarich, J.D. Castillo, D.J. Webb, Chem. Mater. 6 (1994) 93.
[17] A. Mewis, Z. Naturforsch. 33B (1978) 382.
[18] A. Mewis, Z. Naturforsch. 34B (1979) 921.

[19] A. Artmann, A. Mewis, M. Roepke, G. Michels, Z. Anorg. Allg. Chem. 622 (1996) 679.
[20] P. Wollesen, W. Jeitschko, M. Brylak, L. Dietrich, J. Alloys Compd. 245 (1996) 5.
[21] G. Savelsberg, H. Schäfer, Z. Naturforsch. 33B (1978) 370.
[22] G. Cordier, H. Schäfer, M. Stelter, Z. Anorg. Allg. Chem. 519 (1984) 183.
[23] S.-M. Park, E.-S. Choi, W. Kang, S.-J. Kim, J. Mater. Chem. 12 (2002) 1839.